Response of large-scale ionospheric convection to substorm expansion onsets: A case study

Y. Miyashita,[1] K. Hosokawa,[2] T. Hori,[3] Y. Kamide,[4] A. S. Yukimatu,[5] M. Fujimoto,[1] T. Mukai,[1] S. Machida,[6] N. Sato,[5] Y. Saito,[1] I. Shinohara,[1] and J. B. Sigwarth[7]

Received 7 July 2008; revised 22 September 2008; accepted 20 October 2008; published 20 December 2008.

[1] We have studied the response of large-scale ionospheric convection to substorm expansion onsets on the basis of two weak substorms of 1 May 2001, during which a large part of the dawn cell of the two-cell ionospheric convection pattern was monitored by the SuperDARN radars. Ionospheric convection began to enhance first in a localized region of the equatorward part of the dawn cell ~2 minutes before the expansion onsets of both substorms and then enhanced in the entire dawn cell successively. The enhanced convection persisted throughout their expansion phase, possibly even near the footprint of a plasma sheet region without fast flows observed by Geotail. These observations suggest that ionospheric convection begins to enhance just before substorm expansion onset and then enhances in the entire cell, possibly regardless of the presence of fast earthward flows in the corresponding plasma sheet region of the magnetotail. The global enhancement of ionospheric convection is consistent with that of magnetotail convection, which also begins just before onset.

Citation: Miyashita, Y., et al. (2008), Response of large-scale ionospheric convection to substorm expansion onsets: A case study, *J. Geophys. Res.*, *113*, A12309, doi:10.1029/2008JA013586.

1. Introduction

[2] A substorm is a global energy dissipation process in near-Earth space. Various phenomena associated with substorm expansion onsets occur in the magnetosphere, in the ionosphere, and on the ground with causal relationships with each other. Manifestations of substorm-associated phenomena are observed by different spacecraft and ground-based instruments.

[3] One of the most outstanding and unresolved problems in substorm research is the triggering mechanism of an expansion onset. Various models have been proposed [e.g., *Smith et al.*, 1986; *Rostoker and Eastman*, 1987; *Kan et al.*, 1988; *Lyons*, 1995; *Baker et al.*, 1996; *Lui*, 1996]. Among them, changes in convection are proposed as an important factor for causing an expansion onset: large-scale reduction [*Lyons*, 1995] or localized enhancement [*Kan and Sun*, 1996]. Hence it is crucial to study how convection responds to a substorm expansion onset.

[4] On the basis of observations from ground-based instruments, such as SuperDARN radars and magnetometers, a number of previous studies have examined changes in ionospheric convection or flow in association with substorm onset. The response as well as its timing, however, is very controversial: Some previous studies concluded that ionospheric convection reduces at or just before onset. For example, *Lyons et al.* [2001, 2003] reported that ionospheric convection reduces significantly a few minutes before onset on the dayside as well as on the duskside. *Jayachandran et al.* [2003] reported that ionospheric convection gradually weakens during the growth phase and further weakens after onset on the dayside and in the polar cap. *Bristow et al.* [2001, 2003] and *Bristow and Jensen* [2007] reported that ionospheric convection enhances during the growth phase but it reduces at onset. In contrast, some other previous studies concluded that ionospheric convection enhances at onset [e.g., *Kamide et al.*, 1996; *Opgenoorth and Pellinen*, 1998; *Grocott et al.*, 2002, 2006; *Liang et al.*, 2004, 2006; *Provan et al.*, 2004]. *Borälv et al.* [2000] and *Saka et al.* [2001] reported that ionospheric convection may enhance a few minutes before onset. *Kepko et al.* [2004] showed that convection enhanced in the midnight sector a few minutes before onset.

[5] In the magnetotail, convection enhances in association with substorm onset. *Miyashita et al.* [2000, 2001, 2003] and S. Machida et al. (preprint, 2008) showed that the equatorward plasma flow and Poynting flux, and the duskward electric field enhance in the entire lobe regions; the enhancements begin a few minutes before onset.

[1]Institute of Space and Astronautical Science, Japan Aerospace Exploration Agency, Sagamihara, Kanagawa, Japan.
[2]Department of Information and Communication Engineering, University of Electro-Communications, Chofu, Tokyo, Japan.
[3]Solar-Terrestrial Environment Laboratory, Nagoya University, Nagoya, Aichi, Japan.
[4]Research Institute for Sustainable Humanosphere, Kyoto University, Uji, Kyoto, Japan.
[5]National Institute of Polar Research, Itabashi, Tokyo, Japan.
[6]Department of Geophysics, Kyoto University, Kyoto, Japan.
[7]Goddard Space Flight Center, NASA, Greenbelt, Maryland, USA.

Copyright 2008 by the American Geophysical Union.
0148-0227/08/2008JA013586

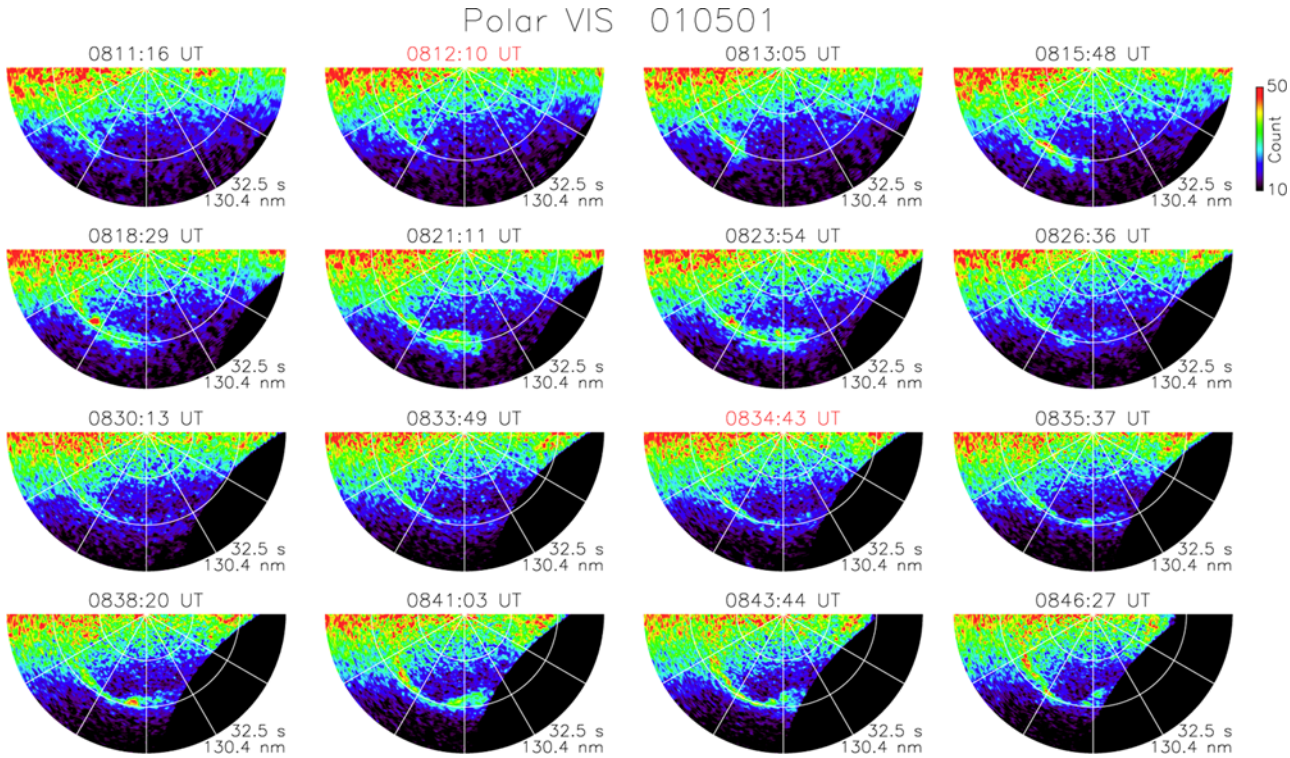

Figure 1. Selected nightside auroral images for the northern hemisphere obtained from the Earth camera of Polar VIS from 0811 to 0847 UT on 1 May 2001, showing the substorm expansion onsets at 0812:16 UT ±27 seconds (labeled 0812:10 UT) and at 0834:49 UT ±27 seconds (labeled 0834:43 UT). The magnetic midnight (0 hours MLT) and dusk (18 hours MLT) are plotted to the bottom and left, respectively. The contours of AACGM latitudes are drawn every 10°. The data integration period (32.5 seconds) and wavelength (130.4 nm) are shown at the lower right-hand corner of each figure. The time indicated at the top of each figure is the start of data integration period in UT.

Taguchi et al. [2001] also found the enhanced equatorward plasma flow in the lobe near the magnetic reconnection region at onset. In the plasma sheet fast earthward flows are seen around onset [e.g., *Angelopoulos et al.*, 1997; *Petrukovich et al.*, 1998; *Fairfield et al.*, 1999; *Nakamura et al.*, 2001a, 2001b; *Slavin et al.*, 2002], although they are very localized in the *Y* direction [*Angelopoulos et al.*, 1997].

[6] *Kauristie et al.* [2000], *Grocott et al.* [2004], and *Nakamura et al.* [2005] have shown that microscopically, twin small-scale vortices are generated in the ionosphere, corresponding to a fast earthward flow, or plasma bubble, in the plasma sheet of the magnetotail. They are connected by field-aligned currents, as a small-scale current wedge; that is, the dawnside and duskside of a flow in the plasma sheet are connected to downward and upward field-aligned currents, respectively.

[7] In the present study, we have investigated in detail two substorm events that occurred on 1 May 2001. During these events, SuperDARN observations covered a large part of the dawn cell of the two-cell convection pattern, lying near the onset sites. The Geotail spacecraft was located in the plasma sheet, whose footprint was in the equatorward part of the dawn cell. Geotail observed successive fast earthward flows only during the second substorm. Hence these events are good for studying the response of ionospheric convection to substorm expansion onsets as well as fast earthward flows in the magnetotail.

2. Observations

2.1. Aurora and Geomagnetic Field

[8] Figure 1 shows selected nightside auroral images for the northern hemisphere obtained from the Earth camera of the Polar visible imaging system (VIS) [*Frank et al.*, 1995] in altitude adjusted corrected geomagnetic (AACGM) coordinates [*Baker and Wing*, 1989]. Two auroral breakups, or substorm expansions, occurred during the interval. The first substorm expansion onset was initiated at ~70° AACGM latitude and ~22 hours MLT at 0812:16 UT ±27 seconds (labeled 0812:10 UT). The auroral bulge reached a maximum at ~0823 UT, extending from ~68° to ~73° latitude and from ~21 to ~1.5 hours MLT. The second substorm expansion onset was initiated at ~70° latitude and ~0 hours MLT at 0834:49 UT ±27 seconds (labeled 0834:43 UT). Although the time of the maximum stage and the extension of the auroral bulge cannot definitely be determined simply because the postmidnight sector was gradually moving out of the field of view of the VIS camera, the auroral bulge probably reached a maximum after ~0840 UT and extended from ~69° to ~74° latitude and from ~23 to at least ~1 hour MLT. The onset latitudes of these substorms

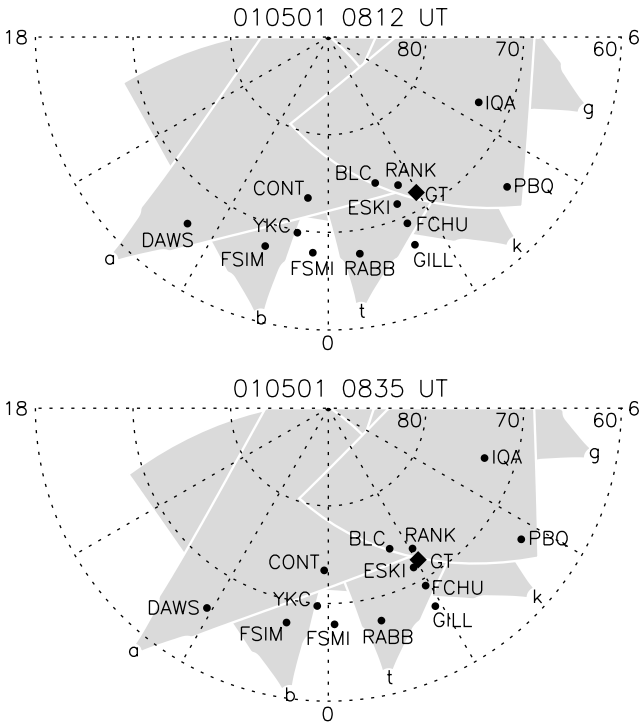

Figure 2. Locations of ground stations (dots), fields of view of SuperDARN radars (light gray areas), and location of the footprint of the Geotail spacecraft (GT, square) in AACGM at the onset times of the two substorms. The stations with four- and three-letter code are of CANOPUS and CANMOS, respectively. The auroral and magnetic field data taken at these stations are shown in Figures 3 and 4. The radar fields of view shown are for Kodiak (denoted by a), Prince George (b), Saskatoon (t), Kapuskasing (k), Goose Bay (g), and Stokkseyri.

were a few degrees higher than typical latitudes of ~66° [e.g., *Craven and Frank*, 1991; *Liou et al.*, 2001].

[9] We also examined the corresponding ground-based auroral and magnetic field data to confirm the substorm onset signatures. The locations of the ground stations are shown in Figure 2, where the stations with four- and three-letter code are of the CANOPUS [*Rostoker et al.*, 1995] and CANMOS stations, respectively.

[10] Figure 3 shows the keograms obtained from the meridian scanning photometers (MSP) for 557.7 nm at Fort Smith (FSMI, ~23 to 0 hours MLT) and Gillam (GILL, ~1 to 2 hours MLT) of CANOPUS with 1 minute resolution. The signatures of the two substorms described above were seen at ~0815 and ~0836 UT with a time delay of a few minutes, although that of the first substorm is not very clear because of clouds. In addition to the two substorms, three weak auroral brightenings or pseudobreakups were observed at ~68° latitude at ~0738, ~0755, and ~0802 UT before the substorms. The exact onset times could not be determined, since these three pseudobreakups could not be identified from the Polar VIS global auroral images, due to the very weak luminosity.

[11] Figure 4 shows the northward component of the geomagnetic field with 5 second resolution at the CANOPUS and CANMOS stations shown in Figure 2. Clear negative perturbations associated with the development of the westward auroral electrojet were observed for both of the two substorms: particularly, Yellowknife (YKC), FSMI, Rabbit Lake (RABB), and Fort Churchill (FCHU) 1 or 2 minutes after the first onset, and Eskimo Point (ESKI) 1 minute after the second onset. The magnitudes of these perturbations were ~100 nT. The positive bays at low and middle latitudes were also observed, consistent with the substorm signatures at high latitudes, although the positive bays were very small for the second substorm (not shown).

[12] According to these auroral and geomagnetic observations, the substorms examined here were weak in terms of the extension of the auroral bulge (~5° in latitude), auroral luminosity, the magnitude of the bay-type perturbations of the geomagnetic field (~100 nT at high latitudes), and the duration of the expansion phase (~10 minutes). Furthermore, note that although the accuracy of the onset times is ~1 minute, they were determined from the global observations of the auroral breakups by Polar VIS, not from other ground and magnetospheric signatures, such as bay-type perturbations and dispersionless injection of energetic particles at geosynchronous orbit. In general, determining an onset time from local observations by ground-based instruments and spacecraft is subject to their locations relative to the true onset site, or the time delay due to the propagation effect [*Liou et al.*, 1999], in spite of their time resolutions that are often higher than those of global auroral observations by spacecraft.

[13] Figure 5 (bottom) shows the 1 minute resolution *Sym-H* index, which is equivalent to the *Dst* index. The *Sym-H* index was ~−10 nT throughout the interval, indicating that the substorms examined here occurred during a nonstorm-time period.

2.2. Solar Wind

[14] Figure 5 also shows the 64 second resolution solar wind parameters and the 16 second resolution interplanetary magnetic field (IMF) measurements obtained from the ACE solar wind electron, proton, and alpha monitor (SWEPAM) and magnetic field experiment (MAG), respectively. The data are shifted according to a propagation time from the ACE position of GSM $X \sim 224\ R_E$ to the ionosphere, roughly estimated to be ~66 minutes [cf., *Khan and Cowley*, 1999].

[15] After a period of northward IMF, the magnitude of IMF B_z became small, ~1–2 nT, and had several southward excursions after ~6 hours UT. The B_y component remained duskward during the events. Hence the IMF was directed nearly duskward from ~6 to ~9 hours UT, i.e., from a few hours before the substorm onsets to the expansion phases (see also the polar angle). The solar wind number density remained extremely low, ~1 cm^{-3}, throughout the interval, resulting in a low dynamic pressure of ~0.3 nPa. There were no significant changes of the solar wind and the IMF at the substorm expansion onsets (the two vertical lines), although there were small fluctuations and somewhat clear changes of B_x and B_z at the second substorm onset.

2.3. Near-Earth Magnetotail

[16] Geotail was located in the postmidnight sector of the near-Earth magnetotail at $(X, Y) \sim (-14, -8)\ R_E$. According

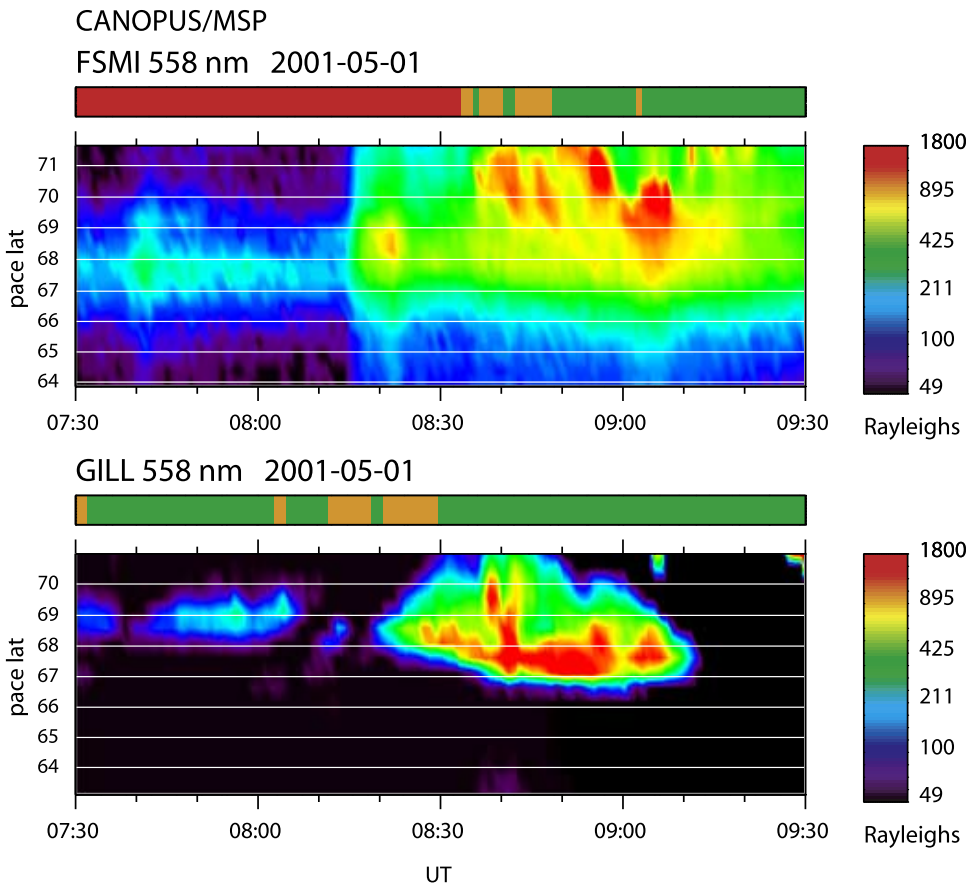

Figure 3. Keograms obtained from the meridian scanning photometers for 557.7 nm at Fort Smith (FSMI) and Gillam (GILL) of CANOPUS from 0730 to 0930 UT on 1 May 2001. The data have a time sampling of 1 minute and are divided into 17 latitude bins. Colors in the horizontal bar above each plot indicate information about clouding: green, red, and orange indicate clear, cloudy, and unknown, respectively.

to the geomagnetic field model T96 by *Tsyganenko* [1995], the footprints of Geotail at the substorm onsets were at ~72° AACGM latitude and ~2.0 hours MLT (see Figure 2), ~4 and ~2 hours eastward of the auroral onset sites of the first and second substorms, respectively. The substorm signatures reached near the Geotail footprint, i.e., FCHU and ESKI 1 or 2 minutes after the onsets for both substorms. The Geotail footprint was located near the edge of or just eastward and poleward of the auroral bulge for the first substorm, while it was located very close to ESKI, where the clear negative perturbation was observed, for the second substorm (Figures 1, 2, and 4).

[17] Figure 6 shows the ion moments and the magnetic field in GSM coordinates obtained from the low-energy particle experiment (LEP) [*Mukai et al.*, 1994] and the magnetic field experiment (MGF) [*Kokubun et al.*, 1994] onboard Geotail with 12 and 3 second resolution, respectively, during the 2 hour interval of 0730 to 0930 UT on 1 May 2001. Geotail remained in the northern plasma sheet throughout the interval, as indicated by the small, positive B_x and the high ion β. The ion number density was lower, and the ion temperature was higher than typical values, ~0.3 cm^{-3} and ~4 keV [see *Baumjohann et al.*, 1989].

[18] For the first substorm, no fast plasma flows were observed, except an earthward flow at ~200 km/s just before the onset. The northward B_z slightly increased ~1 minute after the onset, but it is not clear whether or not this increase related to dipolarization. These observations may well be because Geotail was located near the edge of or just outside the dipolarization region. However, the total pressure, which is the sum of the ion thermal and magnetic pressures, can change in the entire magnetotail, i.e., even outside the active region [e.g., *Miyashita et al.*, 2000, 2008]. In fact, the total pressure clearly decreased ~4 minutes after the onset (Here the contribution of high-energy particles to the ion pressure, measured by the supra-thermal ion composition spectrometer (STICS) of the energetic particles and ion composition instrument (EPIC) [*Williams et al.*, 1994], was neglected, since it was only less than 1% or a few % at most throughout the interval).

[19] For the second substorm, a very clear dipolarization was observed just after the onset, with rapid magnetic field fluctuations. This dipolarization was accompanied by several successive fast earthward flows nearly perpendicular to the ambient magnetic field from ~1 minute after the onset to 0904 UT, which had peaks of ~300 to 1400 km/s and durations of ~2 to 3 minutes. The Y and Z components of the plasma flow were also large and rapidly varied; their perpendicular components were dawnward and toward the

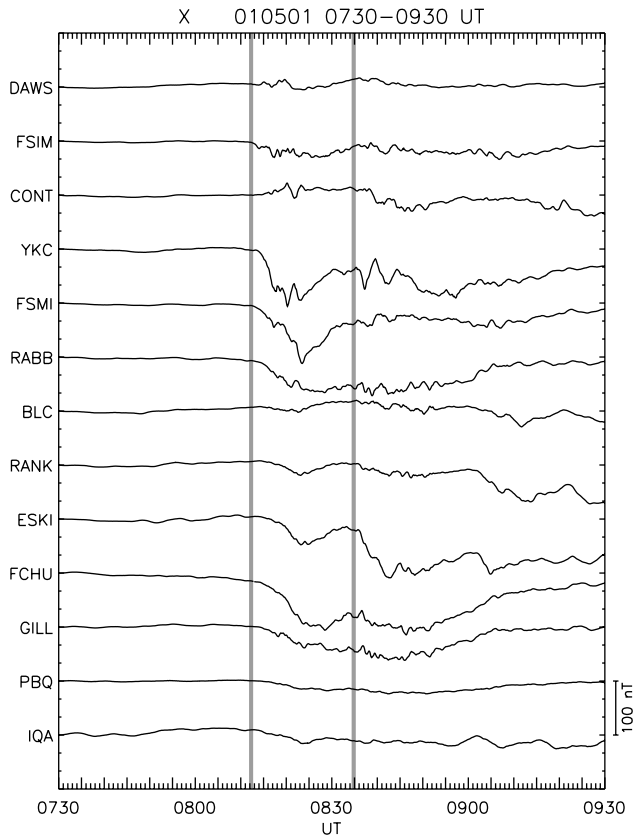

Figure 4. Geographic northward component of the geomagnetic field at the CANOPUS and CANMOS stations shown in Figure 2 from 0730 to 0930 UT on 1 May 2001. The vertical lines indicate the substorm expansion onsets determined from the Polar VIS data.

magnetic equator. The total pressure gradually increased during the dipolarization.

[20] At geosynchronous orbit, GOES 10 observed a dipolarization at ~23.2 hours MLT at the first substorm onset; GOES 8 observed a dipolarization at ~3.6 hours MLT ~1 minute after the second substorm onset (not shown).

2.4. Ionospheric Convection

[21] Next we examined the change in ionospheric convection associated with the substorm onsets. Figure 7 shows selected nightside ionospheric convection maps for the northern hemisphere, obtained from the map potential fitting (eighth-order expansion) [*Ruohoniemi and Baker*, 1998] using SuperDARN [*Greenwald et al.*, 1995] data. During the interval of interest, the SuperDARN radars were operated in a normal scan mode with a high time resolution, in which the radar completes scanning the entire field of view in 1 minute; thus the time resolution of the convection map shown in Figure 7 is 1 minute. Note that we also examined line-of-sight velocities, but the results mentioned below are almost the same. The locations and fields of view of the nightside radars are shown in Figure 2. The radar echoes from the ionosphere were distributed mainly from the midnight to the dawn sectors, so that a large part of the dawn cell of the two-cell ionospheric convection pattern was covered by the real observations during the present events. The echoes did not exist just at the auroral onset sites but were distributed in the close vicinity of them. There were not many echoes on the dayside although the fields of view of two radars covered there and we used their data for the fitting.

[22] For both the first (0812:16 UT ±27 seconds) and second (0834:49 UT ±27 seconds) substorms, ionospheric convection began to enhance first in the equatorward part of the dawn cell at ~1 to ~4 hours MLT just before the expansion onsets, or at 0810 and 0832 UT, respectively, and then enhanced in the entire dawn cell successively. The enhanced convection persisted during the expansion phases. It is interesting to note that very fast flows were not seen in the vicinity of the onset sites within a few minutes of the onsets.

[23] For checking the timing of the convection enhancements, Figure 8 shows the average and maximum ionospheric convection flow speeds for six different 1-hour MLT bins between 65° and 75° AACGM latitude. Here the flow directions are not considered. As indicated by the red triangles, the average and maximum flows began to enhance ~2 minutes before the onset in the midnight to postmidnight sectors at 23 to 4 hours MLT for the first substorm. For the second substorm, the flows began to enhance ~2 minutes before the onset in the postmidnight sector at 2 to 4 hours MLT and then enhanced at other MLTs. The flows near the onset sites, i.e., at ~22 and ~0 hours MLT for the first and second substorms, respectively, began to enhance just after onset (not shown for 22 hours MLT), although the number of the echoes was not very large there, as seen in Figure 7. The enhanced flows generally persisted during the expansion phases, although small variations were seen at some MLTs. The flows began to be quenched around the maximums of the expansion phases.

[24] The ionospheric flows also became strong even during the weak auroral brightenings or pseudobreakups at ~0738, ~0755, and ~0802 UT. As shown in Figure 8, the flows were generally stronger for the pseudobreakups than for the weak substorms. The exact timing of the flow enhancement relative to the pseudobreakup onsets could not be determined, since the exact onset times of the three pseudobreakups could not be determined from the Polar VIS global auroral images.

[25] We compared the ionospheric flows with the plasma flows in the magnetotail during the substorms. Figure 9 shows the average and maximum ionospheric convection flow speeds near the Geotail footprint (±2.5° latitude and ±0.5 hours MLT, in the quadrangular region shown in Figure 7) observed by the SuperDARN radars, and the X component of the plasma flow velocity in the magnetotail observed by Geotail. For the first substorm, Geotail did not observe very fast flows during the expansion phase, but the ionospheric flows enhanced near the Geotail footprint, associated with the expansion onset. As mentioned above, the ionospheric flows also enhanced in the entire dawn cell. For the second substorm, however, Geotail observed several successive fast earthward flows during the expansion phase. Ionospheric flows enhanced not only near the Geotail footprint but also in the entire dawn cell. Twin small-scale vortices are expected to

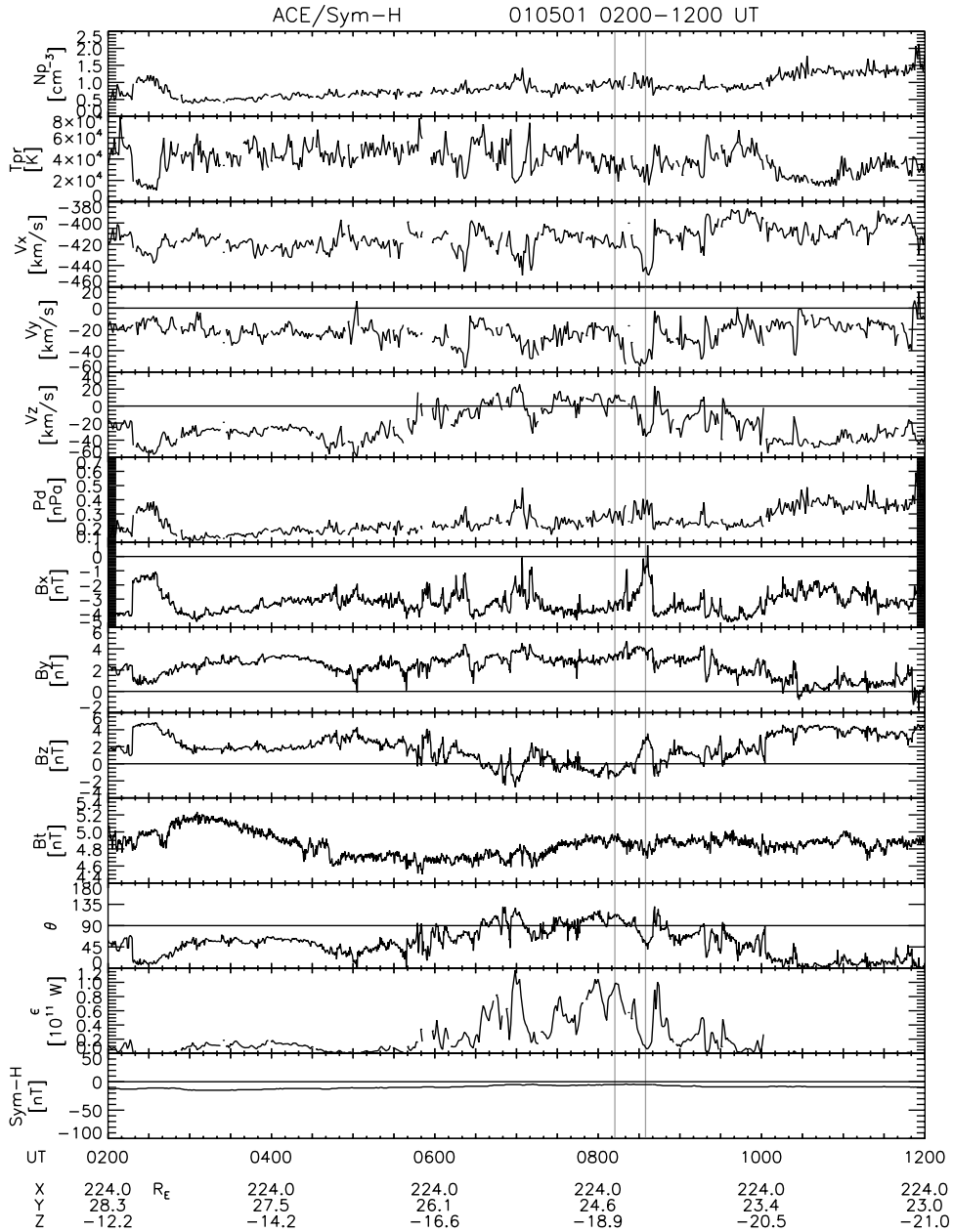

Figure 5. Solar wind parameters (the proton number density, the proton temperature, the three components of the velocity, and the proton dynamic pressure), the interplanetary magnetic field (the three components, the total field, and the polar angle θ), and the epsilon parameter ε obtained by ACE in GSM coordinates, and the *Sym-H* index from 0200 UT to 1200 UT on 1 May 2001. The polar angles of the magnetic field 0°, 90°, and 180° correspond to the northward, dawn-dusk, and southward directions, respectively. The ACE data are shifted according to a propagation time from the ACE position to the ionosphere, ~66 minutes. The vertical lines indicate the substorm expansion onsets determined from the Polar VIS data.

appear eastward and westward of the Geotail footprint, corresponding to a fast earthward flow in the plasma sheet, but such vortices do not seem to be seen (Figure 7). One-to-one correspondence between the flows at Geotail and near its footprint is not clearly seen in Figure 9, probably because of the different time resolutions of the data, i.e., 12 seconds for Geotail and 1 minute for SuperDARN. These observations suggest that ionospheric flows enhance not only near the footprint of a fast flow in the magnetotail but also in the entire cell during the substorm expansion phase. This will be further discussed later.

[26] We also checked line-of-sight and merged SuperDARN velocities (not shown) and found that they varied almost in the same way as the map potential velocities. These consistent results indicate that the observed flow enhancements are real.

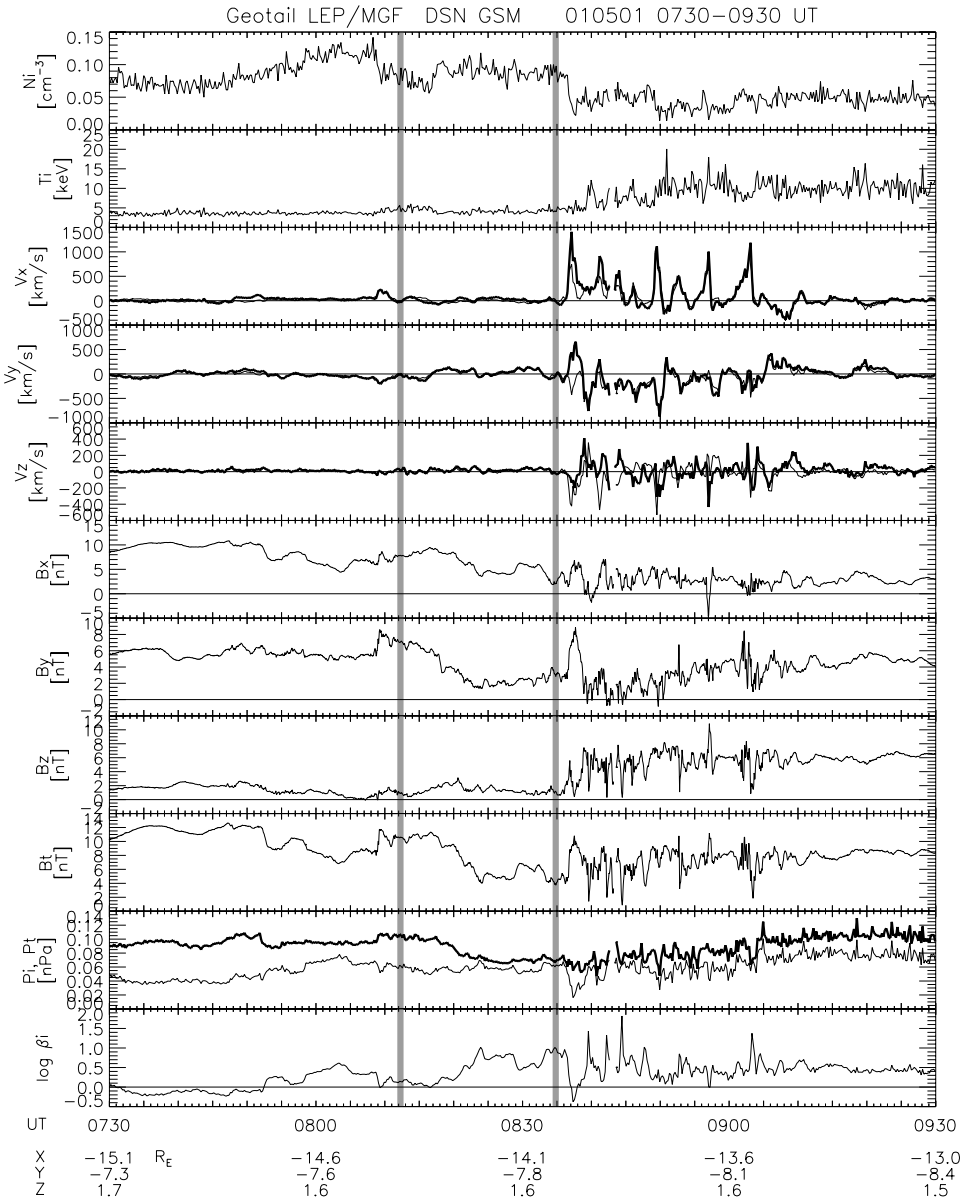

Figure 6. The ion number density, the ion temperature, the three components of the ion velocity (thick lines) and the ion velocity perpendicular to the magnetic field (thin lines), the three components of the magnetic field, the total magnetic field, the total (upper thick line) and ion (lower thin line) pressures, and the ion beta obtained by Geotail from 0730 to 0930 UT on 1 May 2001 in GSM coordinates. The vertical lines indicate the substorm expansion onsets determined from the Polar VIS data.

[27] Besides the common feature of the large-scale convection enhancement just before the substorm onsets, there are a few differences in smaller-scale flow change between the first and second substorms. First, the region of stronger flows differs between the two substorms. Namely, as shown in Figure 7, the stronger flows were seen in the equatorward part of the dawn cell for the first substorm, generating the crescent-shaped cell, while they were seen in the westward part as well as the poleward and equatorward parts for the second substorm, generating the more round cell. The strong equatorward flows in the midnight sector during the expansion phases may relate to the nightside "unloading cell" proposed by *Kamide et al.* [1994]. The different flow pattern might have been generated by the presence of fast earthward flows in the magnetotail and the effect of the previous activity. Second, the southeastern part of the dusk cell with a clockwise vortex was located at ~22 and ~23 hours MLT for the first and second substorms, respectively, extended more eastward for the second substorm than for the first substorm, although we cannot definitely conclude because of the poor radar echoes there. This extended part of the dusk cell roughly corresponds to the auroral bulge (see Figure 1), and hence the flows were possibly suppressed because of the auroral precipitation. Fast earthward flows in

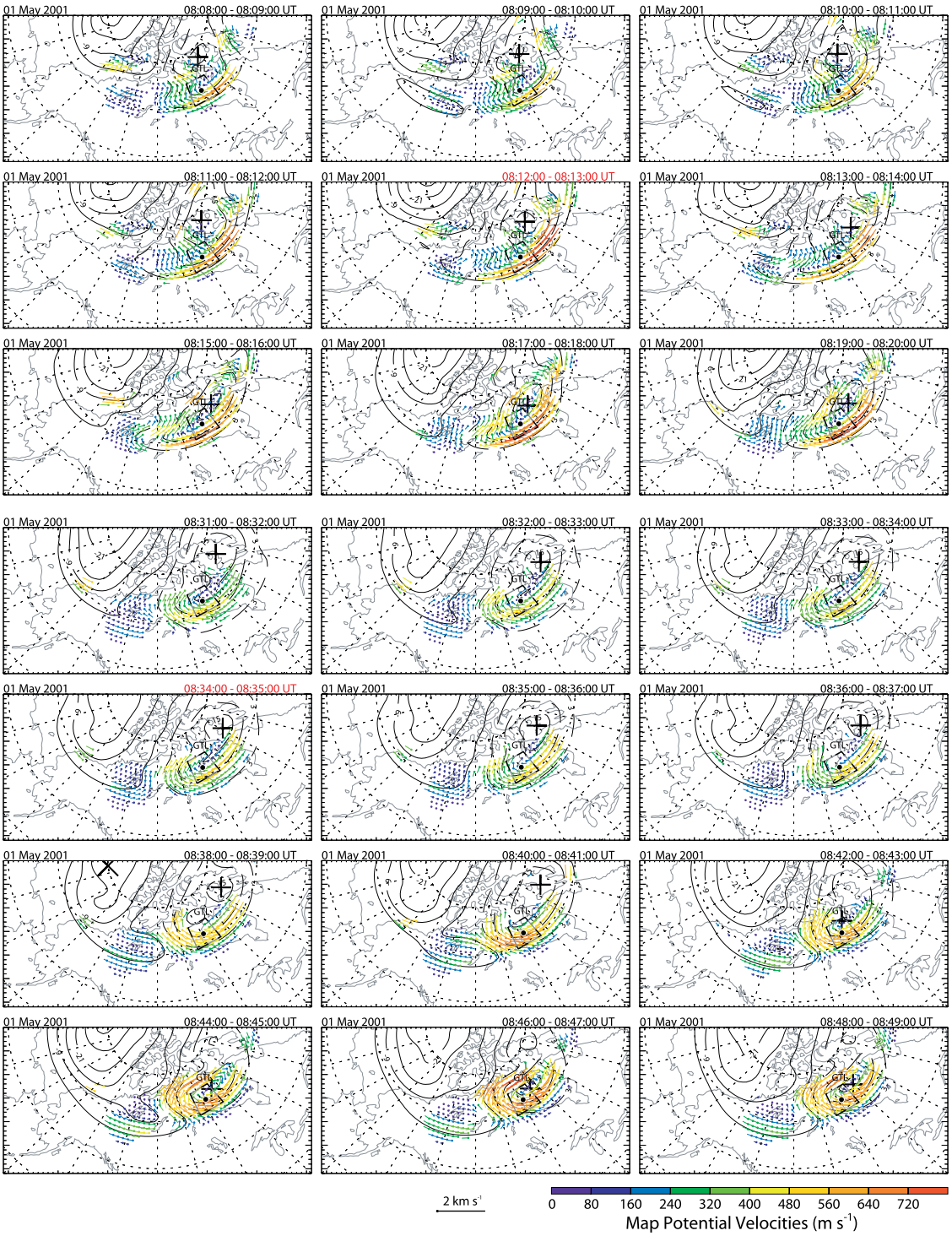

Figure 7. Selected nightside ionospheric convection maps for the northern hemisphere, obtained from the map potential fitting using SuperDARN data with 1 minute resolution for the (top three rows) first (0812:16 UT ±27 seconds) and (bottom four rows) second (0834:49 UT ±27 seconds) substorms. The magnetic midnight (0 hours MLT) and dusk (18 hours MLT) are plotted to the bottom and left, respectively. The contours of AACGM latitudes are drawn every 10°. The dot near ~72° latitude and ~2.0 hours MLT in each figure indicates the footprint of Geotail (GTL). The flows in the quadrangular region (Geotail footprint ±2.5° latitude and ±0.5 hours MLT) are used in Figure 9.

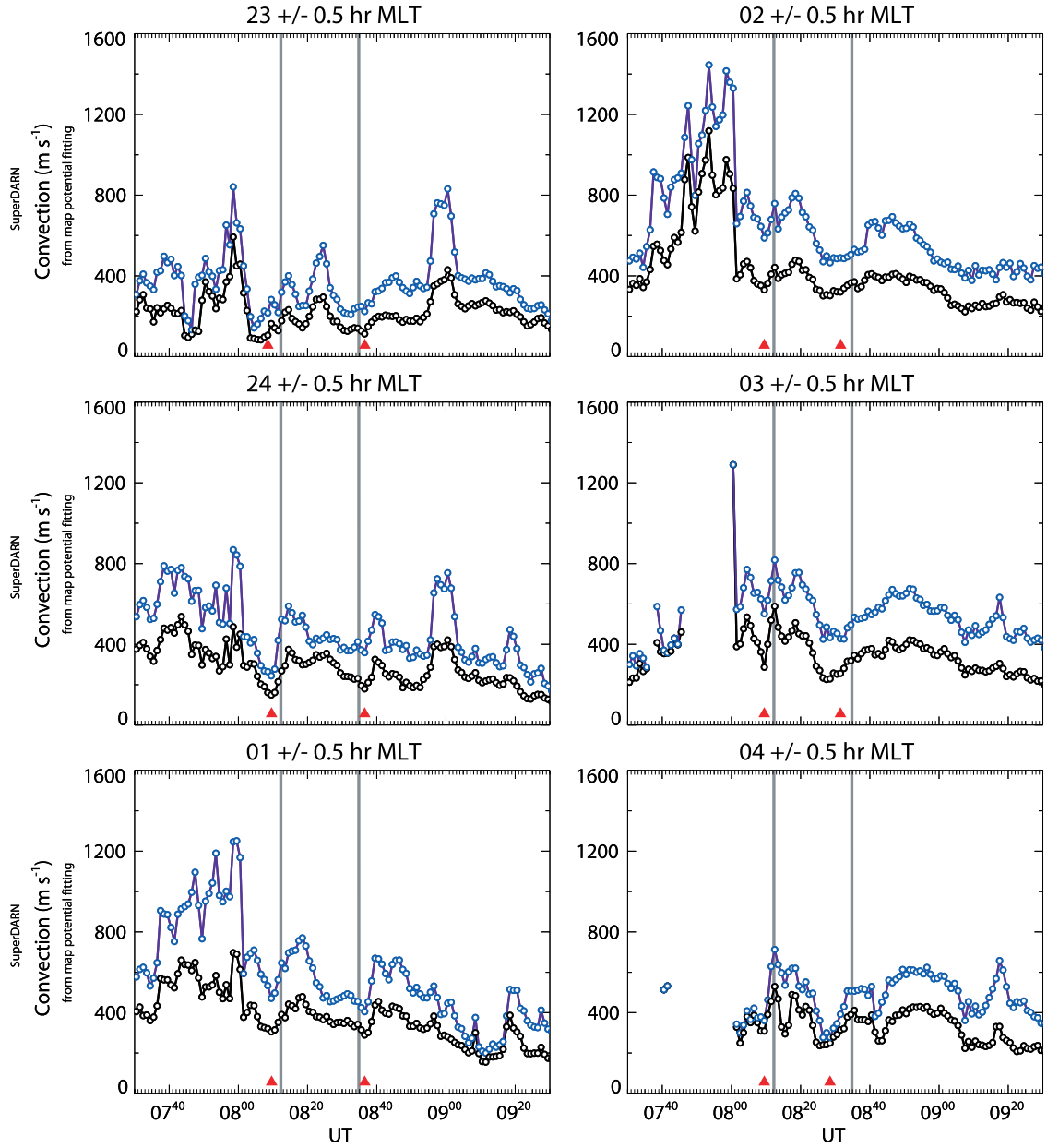

Figure 8. Average (lower black line) and maximum (upper blue line) ionospheric convection flow speeds from 0730 to 0930 UT on 1 May 2001 for six different 1-hour MLT bins between 65° and 75° AACGM latitude, obtained from the SuperDARN radars. The vertical lines indicate the substorm expansion onsets determined from the Polar VIS data. The red triangles indicate the beginnings of the enhancement of the average flow.

the magnetotail may correspond to this region, but we do not have the tail observations for this region.

3. Discussion

[28] We examined in detail the two weak substorms of 1 May 2001 from a viewpoint of the response of ionospheric convection to substorm expansion onsets. During these events a large part of the dawn cell of the two-cell ionospheric convection pattern was monitored by the SuperDARN radars. Ionospheric convection began to enhance first in a localized region of the equatorward part of the dawn cell ~2 minutes before the expansion onsets of both substorms and then enhanced in the entire dawn cell successively. The enhanced convection persisted during the expansion phases, possibly even near the footprint of a plasma sheet region without fast earthward flows observed by Geotail. These observations suggest that ionospheric convection begins to enhance just before substorm expansion onset and then enhances in the entire cell, possibly regardless of the presence of fast earthward flows in the corresponding plasma sheet region of the magnetotail.

[29] The present results are consistent with the previous results of *Kamide et al.* [1996], *Opgenoorth and Pellinen*

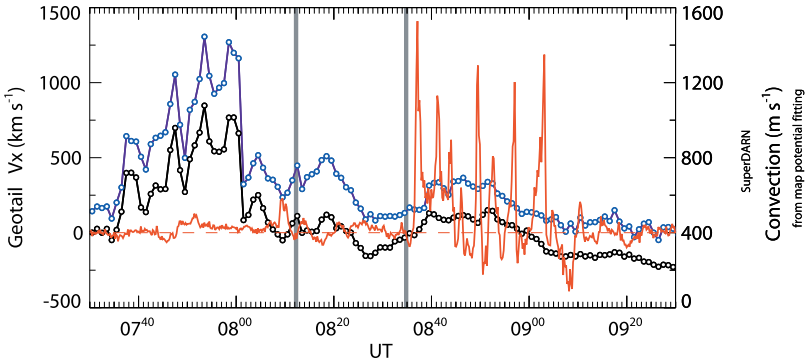

Figure 9. Average (black line with open circles) and maximum (blue line with open circles) ionospheric convection flow speeds near the Geotail footprint (in the quadrangular region, as shown in Figure 7) observed by the SuperDARN radars, and the *X* component of the plasma flow velocity in the magnetotail observed by Geotail (red line without circles) from 0730 to 0930 UT on 1 May 2001. The vertical lines indicate the substorm expansion onsets determined from the Polar VIS data.

[1998], *Borälv et al.* [2000], *Saka et al.* [2001], *Grocott et al.* [2002, 2006], *Liang et al.* [2004, 2006], and *Provan et al.* [2004] in that ionospheric convection enhances, not reduces, in association with substorm onset. In the present study, we examined the timing of the convection change relative to substorm onset in more detail. As mentioned above, we determined the onset times from the global observations of auroral breakups by Polar VIS, not from local observations on the ground or in the magnetosphere as done by, for example, *Opgenoorth and Pellinen* [1998], *Borälv et al.* [2000], and *Saka et al.* [2001]. This means that the onset times determined here are quite accurate, without being subject to the time delay due to the propagation effect [*Liou et al.*, 1999]. Hence, even taking into account the time accuracy of ~1 minute, we can conclude that ionospheric convection begins to enhance just before onset. Although *Kepko et al.* [2004] determined the onset times from global auroral images and showed that convection enhanced in the midnight sector a few minutes before onset, we showed that the convection change occurs also in the dawn sector away from the auroral onset region and bulge, beginning just before onset.

[30] In contrast, the present results are different from those of *Bristow et al.* [2001], *Lyons et al.* [2003], and *Bristow and Jensen* [2007], who suggested from SuperDARN data that ionospheric convection reduces just before or at onset. We therefore attempted to reexamine their events for which global auroral images from the Polar ultraviolet imager (UVI) or the IMAGE far ultraviolet imager (FUV) were available to determine the onset times. We found that ionospheric convection generally appears to enhance just before onset, as observed in the present events.

[31] Possible reasons for the discrepancy are as follows: First, in the previous studies, the onset times for some of the events were determined from ground data, causing a delay of several minutes, so that the changes associated with the true onsets must have been missed. Second, the reduction of flows may be caused by a local effect; that is, flows are suppressed in the auroral bulge [*Provan et al.*, 2004], because of the high conductivity, compared to the surrounding regions. Third, echoes for strong flows may suddenly disappear just around onset, for example, due to absorption of radio waves in strong auroral precipitation regions, which could give false flow reductions. Fourth, it is probable that flows are slowed when the IMF turns northward. Some flows, however, were seen to enhance at the time of substorm onset in the events of *Lyons et al.* [2003]. The behavior of flows may depend on which effect is dominant, the IMF northward turning or the substorm expansion onset. More detailed study should be done in the future to understand the behavior of flows in various regions under different solar wind/IMF conditions.

[32] *Lyons* [1995] proposed that the reduction of large-scale convection leads to the substorm onset. However, this model is not compatible with our results. Meanwhile, *Kan and Sun* [1996] predict that a localized convection enhancement in the onset region is necessary for the substorm triggering. In the present events the SuperDARN observations did not cover directly the onset regions, so that we cannot draw a conclusion of whether such a localized enhancement appears. It seems likely, however, that convection enhancement just before onset is not localized, but global.

[33] It is not likely that in the present events, the convection change just before onset was due to IMF changes. Convection usually enhances when the polar angle of the IMF becomes large and the IMF becomes more southward [*Ridley et al.*, 1998; *Ruohoniemi and Greenwald*, 1998]. As shown in Figure 5, however, the IMF did not become more southward around the first substorm onset and was even northward around the second substorm. Also, the dynamic pressure, which may be a possible factor for convection change, did not change significantly around the onsets.

[34] Interestingly, ionospheric convection enhanced at the onsets of the pseudobreakups (pseudosubstorms). Pseudosubstorms are quite similar to substorms, probably caused by the same physical process, but are generally weaker, more localized, and more short-lived than substorms, without subsequent large-scale development. It is possible that their development is suppressed by some mechanism, or magnetospheric or ionospheric conditions are not favorable

for full-scale development. The convection enhancements in the present events can suggest that the same processes work at the onsets of pseudosubstorms and substorms. Meanwhile, the ionospheric flows were generally stronger for the pseudobreakups than for the weak substorms (Figure 8). This difference might be generated by the spatial scale and intensity of the auroral breakup as well as background disturbed/undisturbed conditions around onsets. This is, however, an open question.

[35] It is often thought that ionospheric flows are connected with fast flows in the plasma sheet of the magnetotail and inner magnetosphere, as mentioned in the Introduction. The present events, however, demonstrate that this is not always the case, that is, ionospheric flows can enhance even without corresponding fast flows in the plasma sheet. The first substorm event showed that ionospheric convection enhanced at least in the entire dawn cell although Geotail did not observe very fast flows in the plasma sheet after the onset. It was also shown that fast earthward flows are very localized in the *Y* direction [*Angelopoulos et al.*, 1997]. Hence we suggest from these results that the global enhancement of ionospheric convection is not driven by localized fast flows in the plasma sheet, but driven by more global phenomena caused by magnetic reconnection and dipolarization. Note that Geotail possibly missed fast flows even in the plasma sheet, or the Geotail location may be mapped to a region of very slow ionospheric flows. This issue should be further examined on the basis of multispacecraft observations.

[36] The global enhancement of ionospheric convection that we have found in the present study is consistent with the global changes in the magnetotail. *Miyashita et al.* [2000, 2003, 2008] statistically showed that magnetic reconnection and dipolarization occur in the magnetotail a few minutes before auroral onset. As a result of these processes in the plasma sheet, convection or the duskward electric field enhances first in a localized region of the lobe and then enhances in the entire lobe successively [*Miyashita et al.*, 2000, 2003; S. Machida et al., preprint, 2008]. The convection enhancement can be seen widely in the lobe, in contrast to localized fast flows in the plasma sheet. Hence ionospheric convection change may be a manifestation of these global magnetotail changes, with a possible response time within 1 or 2 minutes.

[37] It is quite possible that the global enhancement of ionospheric convection is driven by the enhancement of the large-scale field-aligned currents in the ionosphere, which are downward in the dawn cell, i.e., the "region 1" current. In the magnetotail, there is a large-scale field-aligned current system with the polarity consistent with the region 1 current system [*Ohtani et al.*, 1988; *Kaufmann et al.*, 2003]. *Fujimoto et al.* [2001] and *Ueno et al.* [2002] showed that the field-aligned current enhances at the outer edge of the plasma sheet boundary layer in association with substorm or magnetic reconnection, which is interpreted as the Hall current system generated by magnetic reconnection in the midtail. It is, however, an open question how the large-scale field-aligned currents in the entire magnetotail develop around substorm onset and are connected with the ionospheric current system.

[38] Finally, simulations showed that convection plays an important role in the formation of the thin current sheet in the magnetotail [*Pritchett and Coroniti*, 1994; *Cai et al.*, 1995; *Hesse et al.*, 1996; *Tanaka*, 2000], necessary for causing some instability, or magnetic reconnection and current disruption. The enhancement of convection may make further development of the substorm processes. It is also proposed that a localized ionospheric field-aligned current can result in a localized, thin current sheet in the magnetotail [*Pritchett and Coroniti*, 2007]. More details about the causal relationship among magnetospheric and ionospheric convection, field-aligned currents, and substorm triggering processes should be investigated in the future.

[39] **Acknowledgments.** We thank S. Kokubun and T. Nagai for providing the Geotail MGF magnetic field data. We also thank R. W. McEntire, S. P. Christon, and A. T. Y. Lui for the Geotail EPIC-STICS high-energy particle data and M. Nosé, D. Nagata, and Y. Ono for preparing them. The ACE SWEPAM plasma data, the ACE MAG magnetic field data, and the GOES magnetic field data were provided by D. J. McComas, N. Ness, and H. J. Singer, respectively, through the Coordinated Data Analysis Web (CDAWeb) at NASA. The CANOPUS MSP auroral data were provided by F. Creutzberg and E. Donovan, and the CANOPUS and CANMOS geomagnetic field data were provided by I. Mann and D. Boteler, respectively, through the Canadian Space Science Data Portal (CSSDP). The *Sym-H* and *Dst* indices were provided by World Data Center for Geomagnetism, Kyoto. The Polar UVI auroral imager data were provided by K. Liou and G. K. Parks. The IMAGE FUV auroral imager data were provided by S. B. Mende. We thank all the staff who contributed to the operation of the SuperDARN radars. We also thank F. Creutzberg for his useful comments. This research was supported in part at the University of Iowa by the National Aeronautics and Space Administration under NAG5-11528.

[40] Wolfgang Baumjohann thanks Jun Liang and another reviewer for their assistance in evaluating this paper.

References

Angelopoulos, V., et al. (1997), Magnetotail flow bursts: Association to global magnetospheric circulation, relationship to ionospheric activity and direct evidence for localization, *Geophys. Res. Lett.*, *24*(18), 2271–2274.

Baker, K. B., and S. Wing (1989), A new magnetic coordinate system for conjugate studies at high latitudes, *J. Geophys. Res.*, *94*(A7), 9139–9143.

Baker, D. N., T. I. Pulkkinen, V. Angelopoulos, W. Baumjohann, and R. L. McPherron (1996), Neutral line model of substorms: Past results and present view, *J. Geophys. Res.*, *101*(A6), 12,975–13,010.

Baumjohann, W., G. Paschmann, and C. A. Cattell (1989), Average plasma properties in the central plasma sheet, *J. Geophys. Res.*, *94*(A6), 6597–6606.

Borälv, E., P. Eglitis, H. J. Opgenoorth, E. Donovan, G. Reeves, and P. Stauning (2000), The dawn and dusk electrojet response to substorm onset, *Ann. Geophys.*, *18*(9), 1097–1107.

Bristow, W. A., and P. Jensen (2007), A superposed epoch study of SuperDARN convection observations during substorms, *J. Geophys. Res.*, *112*, A06232, doi:10.1029/2006JA012049.

Bristow, W. A., A. Otto, and D. Lummerzheim (2001), Substorm convection patterns observed by the Super Dual Auroral Radar Network, *J. Geophys. Res.*, *106*(A11), 24,593–24,609.

Bristow, W. A., G. J. Sofko, H. C. Stenbaek-Nielsen, S. Wei, D. Lummerzheim, and A. Otto (2003), Detailed analysis of substorm observations using SuperDARN, UVI, ground-based magnetometers, and all-sky imagers, *J. Geophys. Res.*, *108*(A3), 1124, doi:10.1029/2002JA009242.

Cai, H. J., L. C. Lee, and L. Zhang (1995), Tailward stretching of geomagnetic field lines in the presence of an enhanced ionospheric convection electric field, *Geophys. Res. Lett.*, *22*(24), 3449–3452.

Craven, J. D., and L. A. Frank (1991), Diagnosis of auroral dynamics using global auroral imaging with emphasis on large-scale evolutions, in *Auroral Physics*, edited by C.-I. Meng, M. J. Rycroft, and L. A. Frank, pp. 273–288, Cambridge Univ. Press, New York.

Fairfield, D. H., et al. (1999), Earthward flow bursts in the inner magnetotail and their relation to auroral brightenings, AKR intensifications, geosynchronous particle injections and magnetic activity, *J. Geophys. Res.*, *104*(A1), 355–370.

Frank, L. A., J. B. Sigwarth, J. D. Craven, J. P. Cravens, J. S. Dolan, M. R. Dvorsky, P. K. Hardebeck, J. D. Harvey, and D. W. Muller (1995), The Visible Imaging System (VIS) for the Polar spacecraft, *Space Sci. Rev.*, *71*(1-4), 297–328.

Fujimoto, M., T. Nagai, N. Yokokawa, Y. Yamade, T. Mukai, Y. Saito, and S. Kokubun (2001), Tailward electrons at the lobe-plasma sheet interface detected upon dipolarizations, *J. Geophys. Res.*, *106*(A10), 21,255–21,262.

Greenwald, R. A., et al. (1995), DARN/SuperDARN: A global view of the dynamics of high-latitude convection, *Space Sci. Rev.*, *71*(1–4), 761–796.

Grocott, A., S. W. H. Cowley, J. B. Sigwarth, J. F. Watermann, and T. K. Yeoman (2002), Excitation of twin-vortex flow in the nightside high-latitude ionosphere during an isolated substorm, *Ann. Geophys.*, *20*(10), 1577–1601.

Grocott, A., T. K. Yeoman, R. Nakamura, S. W. H. Cowley, H. U. Frey, H. Rème, and B. Klecker (2004), Multi-instrument observations of the ionospheric counterpart of a bursty bulk flow in the near-Earth plasma sheet, *Ann. Geophys.*, *22*(4), 1061–1075.

Grocott, A., M. Lester, M. L. Parkinson, T. K. Yeoman, P. L. Dyson, J. C. Devlin, and H. U. Frey (2006), Towards a synthesis of substorm electrodynamics: HF radar and auroral observations, *Ann. Geophys.*, *24*(12), 3365–3381.

Hesse, M., D. Winske, M. Kuznetsova, J. Birn, and K. Schindler (1996), Hybrid modeling of the formation of thin current sheets in magnetotail configurations, *J. Geomagn. Geoelectr.*, *48*(5-6), 749–763.

Jayachandran, P. T., J. W. MacDougall, E. F. Donovan, J. M. Ruohoniemi, K. Liou, D. R. Moorcroft, and J.-P. St-Maurice (2003), Substorm associated changes in the high-latitude ionospheric convection, *Geophys. Res. Lett.*, *30*(20), 2064, doi:10.1029/2003GL017497.

Kamide, Y., et al. (1994), Ground-based studies of ionospheric convection associated with substorm expansion, *J. Geophys. Res.*, *99*(A10), 19,451–19,466.

Kamide, Y., W. Sun, and S.-I. Akasofu (1996), The average ionospheric electrodynamics for the different substorm phases, *J. Geophys. Res.*, *101*(A1), 99–109.

Kan, J. R., and W. Sun (1996), Substorm expansion phase caused by an intense localized convection imposed on the ionosphere, *J. Geophys. Res.*, *101*(A12), 27,271–27,281.

Kan, J. R., L. Zhu, and S.-I. Akasofu (1988), A theory of substorms: Onset and subsidence, *J. Geophys. Res.*, *93*(A6), 5624–5640.

Kaufmann, R. L., W. R. Paterson, and L. A. Frank (2003), Birkeland currents in the plasma sheet, *J. Geophys. Res.*, *108*(A7), 1299, doi:10.1029/2002JA009665.

Kauristie, K., V. A. Sergeev, M. Kubyshkina, T. I. Pulkkinen, V. Angelopoulos, T. Phan, R. P. Lin, and J. A. Slavin (2000), Ionospheric current signatures of transient plasma sheet flows, *J. Geophys. Res.*, *105*(A5), 10,677–10,690.

Kepko, L., M. G. Kivelson, R. L. McPherron, and H. E. Spence (2004), Relative timing of substorm onset phenomena, *J. Geophys. Res.*, *109*, A04203, doi:10.1029/2003JA010285.

Khan, H., and S. W. H. Cowley (1999), Observations of the response time of high-latitude ionospheric convection to variations in the interplanetary magnetic field using EISCAT and IMP-8 data, *Ann. Geophys.*, *17*(10), 1306–1335.

Kokubun, S., T. Yamamoto, M. H. Acuña, K. Hayashi, K. Shiokawa, and H. Kawano (1994), The Geotail magnetic field experiment, *J. Geomagn. Geoelectr.*, *46*(1), 7–21.

Liang, J., G. J. Sofko, E. F. Donovan, M. Watanabe, and R. A. Greenwald (2004), Convection dynamics and driving mechanism of a small substorm during dominantly IMF By+, Bz+ conditions, *Geophys. Res. Lett.*, *31*, L08803, doi:10.1029/2003GL018878.

Liang, J., G. J. Sofko, and H. U. Frey (2006), Postmidnight convection dynamics during substorm expansion phase, *J. Geophys. Res.*, *111*, A04205, doi:10.1029/2005JA011483.

Liou, K., C.-I. Meng, T. Y. Lui, P. T. Newell, M. Brittnacher, G. Parks, G. D. Reeves, R. R. Anderson, and K. Yumoto (1999), On relative timing in substorm onset signatures, *J. Geophys. Res.*, *104*(A10), 22,807–22,817.

Liou, K., P. T. Newell, D. G. Sibeck, C.-I. Meng, M. Brittnacher, and G. Parks (2001), Observation of IMF and seasonal effects in the location of auroral substorm onset, *J. Geophys. Res.*, *106*(A4), 5799–5810.

Lui, A. T. Y. (1996), Current disruption in the Earth's magnetosphere: Observations and models, *J. Geophys. Res.*, *101*(A6), 13,067–13,088.

Lyons, L. R. (1995), A new theory for magnetospheric substorms, *J. Geophys. Res.*, *100*(A10), 19,069–19,081.

Lyons, L. R., J. M. Ruohoniemi, and G. Lu (2001), Substorm-associated changes in large-scale convection during the November 24, 1996, Geospace Environment Modeling event, *J. Geophys. Res.*, *106*(A1), 397–405.

Lyons, L. R., S. Liu, J. M. Ruohoniemi, S. I. Solovyev, and J. C. Samson (2003), Observations of dayside convection reduction leading to substorm onset, *J. Geophys. Res.*, *108*(A3), 1119, doi:10.1029/2002JA009670.

Miyashita, Y., S. Machida, T. Mukai, Y. Saito, K. Tsuruda, H. Hayakawa, and P. R. Sutcliffe (2000), A statistical study of variations in the near and middistant magnetotail associated with substorm onsets: Geotail observations, *J. Geophys. Res.*, *105*(A7), 15,913–15,930.

Miyashita, Y., S. Machida, T. Mukai, Y. Saito, and P. R. Sutcliffe (2001), Mass and energy transport in the near and middistant magnetotail around substorm onsets: Geotail observations, *J. Geophys. Res.*, *106*(A4), 6259–6274.

Miyashita, Y., et al. (2008), A state-of-the-art picture of substorm-associated evolution of near-Earth magnetotail obtained from superposed epoch analysis, *J. Geophys. Res.*, doi:10.1029/2008JA013225, in press.

Miyashita, Y., S. Machida, K. Liou, T. Mukai, Y. Saito, H. Hayakawa, C.-I. Meng, and G. K. Parks (2003), Evolution of the magnetotail associated with substorm auroral breakups, *J. Geophys. Res.*, *108*(A9), 1353, doi:10.1029/2003JA009939.

Mukai, T., S. Machida, Y. Saito, M. Hirahara, T. Terasawa, N. Kaya, T. Obara, M. Ejiri, and A. Nishida (1994), The low energy particle (LEP) experiment onboard the Geotail satellite, *J. Geomagn. Geoelectr.*, *46*(8), 669–692.

Nakamura, R., W. Baumjohann, M. Brittnacher, V. A. Sergeev, M. Kubyshkina, T. Mukai, and K. Liou (2001a), Flow bursts and auroral activations: Onset timing and foot point location, *J. Geophys. Res.*, *106*(A6), 10,777–10,789.

Nakamura, R., W. Baumjohann, R. Schödel, M. Brittnacher, V. A. Sergeev, M. Kubyshkina, T. Mukai, and K. Liou (2001b), Earthward flow bursts, auroral streamers, and small expansions, *J. Geophys. Res.*, *106*(A6), 10,791–10,802.

Nakamura, R., et al. (2005), Localized fast flow disturbance observed in the plasma sheet and in the ionosphere, *Ann. Geophys.*, *23*(2), 553–566.

Ohtani, S., S. Kokubun, R. C. Elphic, and C. T. Russell (1988), Field-aligned current signatures in the near-tail region 1: ISEE observations in the plasma sheet boundary layer, *J. Geophys. Res.*, *93*(A9), 9709–9720.

Opgenoorth, H. J., and R. J. Pellinen (1998), The reaction of the global convection electrojets to the onset and expansion of the substorm current wedge, in *Proceedings of International Conference on Substorms-4*, edited by S. Kokubun and Y. Kamide, pp. 663–670, Terra Sci., Tokyo.

Petrukovich, A. A., et al. (1998), Two spacecraft observations of a reconnection pulse during an auroral breakup, *J. Geophys. Res.*, *103*(A1), 47–59.

Pritchett, P. L., and F. V. Coroniti (1994), Convection and the formation of thin current sheets in the near-Earth plasma sheet, *Geophys. Res. Lett.*, *21*(15), 1587–1590.

Pritchett, P. L., and F. V. Coroniti (2007), Plasma sheet response to the ionosphere's demand for field-aligned current, *Geophys. Res. Lett.*, *34*, L12104, doi:10.1029/2007GL030245.

Provan, G., M. Lester, S. B. Mende, and S. E. Milan (2004), Statistical study of high-latitude plasma flow during magnetospheric substorms, *Ann. Geophys.*, *22*(10), 3607–3624.

Ridley, A. J., G. Lu, C. R. Clauer, and V. O. Papitashvili (1998), A statistical study of the ionospheric convection response to changing interplanetary magnetic field conditions using the assimilative mapping of ionospheric electrodynamics technique, *J. Geophys. Res.*, *103*(A3), 4023–4039.

Rostoker, G., and T. Eastman (1987), A boundary layer model for magnetospheric substorms, *J. Geophys. Res.*, *92*(A11), 12,187–12,201.

Rostoker, G., J. C. Samson, F. Creutzberg, T. J. Hughes, D. R. McDiarmid, A. G. McNamara, A. Vallance Jones, D. D. Wallis, and L. L. Cogger (1995), CANOPUS-A ground-based instrument array for remote sensing the high latitude ionosphere during the ISTP/GGS program, *Space Sci. Rev.*, *71*(1-4), 743–760.

Ruohoniemi, J. M., and K. B. Baker (1998), Large-scale imaging of high-latitude convection with Super Dual Auroral Radar Network HF radar observations, *J. Geophys. Res.*, *103*(A9), 20,797–20,811.

Ruohoniemi, J. M., and R. A. Greenwald (1998), The response of high-latitude convection to a sudden southward IMF turning, *Geophys. Res. Lett.*, *25*(15), 2913–2916.

Saka, O., T. Kitamura, H. Tachihara, M. Shinohara, N. B. Trivedi, N. Sato, J. M. Ruohoniemi, and R. A. Greenwald (2001), A substorm onset signature at the auroral zone as observed with SuperDARN and equatorial magnetometers, *J. Geophys. Res.*, *106*(A12), 29,037–29,050.

Slavin, J. A., et al. (2002), Simultaneous observations of earthward flow bursts and plasmoid ejection during magnetospheric substorms, *J. Geophys. Res.*, *107*(A7), 1106, doi:10.1029/2000JA003501.

Smith, R. A., C. K. Goertz, and W. Grossmann (1986), Thermal catastrophe in the plasma sheet boundary layer, *Geophys. Res. Lett*, *13*(13), 1380–1383.

Taguchi, S., M. Kiyohara, T. Mukai, M. Nosé, and Y. Saito (2001), Convection enhancements in the low-latitude lobe for substorm onset, *J. Geophys. Res.*, *106*(A3), 3943–3952.

Tanaka, T. (2000), The state transition model of the substorm onset, *J. Geophys. Res.*, *105*(A9), 21,081–21,096.

Tsyganenko, N. A. (1995), Modeling the Earth's magnetospheric magnetic field confined within a realistic magnetopause, *J. Geophys. Res.*, *100*(A4), 5599–5612.

Ueno, G., S. Ohtani, Y. Saito, and T. Mukai (2002), Field-aligned currents in the outermost plasma sheet boundary layer with Geotail observation, *J. Geophys. Res.*, *107*(A11), 1399, doi:10.1029/2002JA009367.

Williams, D. J., R. W. McEntire, C. Schlemm II, A. T. Y. Lui, G. Gloeckler, S. P. Christon, and F. Gliem (1994), Geotail energetic particles and ion composition instrument, *J. Geomagn. Geoelectr.*, *46*(1), 39–57.

M. Fujimoto, Y. Miyashita, T. Mukai, Y. Saito, and I. Shinohara, Institute of Space and Astronautical Science, Japan Aerospace Exploration Agency, 3-1-1 Yoshinodai, Sagamihara, Kanagawa 229-8510, Japan. (miyasita@stp.isas.jaxa.jp)

T. Hori, Solar-Terrestrial Environment Laboratory, Nagoya University, Furo-cho, Chikusa-ku, Nagoya, Aichi 464-8601, Japan.

K. Hosokawa, Department of Information and Communication Engineering, University of Electro-Communications, 1-5-1 Chofugaoka, Chofu, Tokyo 182-8585, Japan.

Y. Kamide, Research Institute for Sustainable Humanosphere, Kyoto University, Gokasho, Uji, Kyoto 611-0011, Japan.

S. Machida, Department of Geophysics, Kyoto University, Kitashirakawa-Oiwake-ocho, Sakyo-ku, Kyoto 606-8502, Japan.

N. Sato and A. S. Yukimatu, National Institute of Polar Research, 1-9-10 Kaga, Itabashi, Tokyo 173-8515, Japan.

J. B. Sigwarth, Goddard Space Flight Center, NASA, Greenbelt, MD 20771, USA.